rotations: A Package for $SO(3)$ Data

by Bryan Stanfill, Heike Hofmann, Ulrike Genschel

Abstract In this article we introduce the **rotations** package which provides users the ability to simulate, analyze and visualize data in $SO(3)$. No package as complete as this one is currently available. We offer four distributions from which to simulate data, four estimators of the central orientation and a novel approach to visualizing these data. All of the above features are available to three different parameterizations of rotations: 3-by-3 matrix form, quaternions and Euler angles.

Introduction

The data in form of three-dimensional rotations find application in several scientific areas, such as biomedical engineering, computer visioning, and geological and materials sciences. A common problem shared by these fields is the estimation of a main or central orientation S. That is, letting the rotation group $SO(3)$ denote the collection of all 3×3 rotation matrices, observations $R_1, \dots, R_n \in SO(3)$ can be conceptualized as a random sample from a *location model*

$$\mathbf{R}_i = SE_i, \quad i = 1, \dots, n, \tag{1}$$

where $S \in SO(3)$ is the *fixed* parameter of interest indicating an orientation of central tendency, and $E_1, \dots, E_n \in SO(3)$ denote iid *random* rotations which symmetrically perturb S.

The **rotations** package allows users to simulate data from four common choices of symmetric distributions, estimate S in 1 and visualize a sample of rotations.

Rotation Representations

The variety of applications for rotations is echoed by the number of equivalent ways to parameterize them. We consider the three of the most popular: 3×3 matrices in $SO(3)$, unit quaternions and Euler angles.

Matrix Form

Given the angle, r, and axis, u, necessary to define a rotation a 3×3 rotation matrix can be formed by

$$R = R(r, u) = uu^\top + (I_{3\times3} - uu^\top)\cos(r) + \Phi(u)\sin(r) \tag{2}$$

where

$$\Phi(u) = \Phi(u_1, u_2, u_3) = \begin{pmatrix} 0 & -u_3 & u_2 \\ u_3 & 0 & -u_1 \\ -u_2 & u_1 & 0 \end{pmatrix}.$$

This is called the axis-angle representation of rotation matrices because R is represented by rotating the coordinate axis $I_{3\times3}$ about the axis $U \in \mathbb{R}^3$ by the angle r. We adopt the material scientist's terminology in calling r the misorientation angle and U the misorientation axis.

Quaternion Form

Quaternions are a form of imaginary numbers with one real entry and a vector of three imaginary parts that can be expressed as

$$q = x_1 + x_2 i + x_3 j + x_4 k$$

where i, j, and k are square roots of -1, i.e. $i^2 = j^2 = k^2 = -1$. We can write $q = (s, v)$ as tuple of the scalar s for coefficient **1** and vector v for the imaginary coefficients, i.e. $s = x_1$ and $v = (x_2, x_3, x_4)$.

A rotation around axis u by angle r translates to $q = (s, v)$ with

$$s = \cos(r/2), \quad v = u \sin(r/2)$$

This makes q a unit quaternion.

This form is popular with mathematicians and others interested in the theory of rotations because their form makes them simple to deal with in certain situations.

Euler Angles

We haven't decided on our favorite form of Euler angles so I will leave this empty for now.

All of the functions in **rotations** will work with any of these representations. For the remainder of this article, however, we will present our work using the matrix representation.

Data generation

Using (1) one can simulate a matrix $E_i \in SO(3)$ by picking an axis u uniformly on the sphere then drawing an angle r from a distribution symmetric about 0 and bounded between $-\pi$ and π then applying (2). A matrix generated in this fashion is said to belong to the *uniform-axis random spin*, or UARS, class of distributions (Bingham et al., 2009). The choice of angular distribution distinguishes between members of this class.

The **rotate** package allows the user access to four members of the UARS class according to four common distributional models on r: the uniform distribution on the sphere, the symmetric matrix Fisher (Langevin, 1905; Downs, 1972; Khatri and Mardia, 1977; Jupp and Mardia, 1979), the symmetric Cayley

(Schaeben, 1997; León et al., 2006) and the circular von Mises-based distribution (Bingham et al., 2009).

The uniform distribution on the sphere is given by the following density function

$$C_H(r) = \frac{1 - \cos(r)}{2\pi}$$

for $r \in (-\pi, \pi]$. This function also plays the part of a measure on the sphere, called the Haar measure on the sphere.

The symmetric matrix Fisher distribution is the oldest and also the most difficult to sample from with the following distributional form

$$C_F(r|\kappa) = \frac{1}{2\pi[I_0(2\kappa) - I_1(2\kappa)]} e^{2\kappa \cos(r)} [1 - \cos(r)]$$

where $I_p(\cdot)$ denotes the Bessel function of order p defined as $I_p(\kappa) = \frac{1}{2\pi} \int_{-\pi}^{\pi} \cos(pr) e^{\kappa \cos r} dr$. The function rfisher generates a sample of size n from this distribution using a rejection algorithm and dfisher evaluates the density at a given angle r.

León et al. (2006) proposed the symmetric Cayley distribution, which is identical to the de la Vallée Poussin distribution and a favorite amongst material scientists (Schaeben, 1997). This distribution is closely related to the beta distribution and has the distributional form

$$C_C(r|\kappa) = \frac{1}{\sqrt{\pi}} \frac{\Gamma(\kappa + 2)}{\Gamma(\kappa + 1/2)} 2^{-(\kappa+1)} (1 + \cos r)^{\kappa} (1 - \cos r).$$

rcayley simulates from this distribution by taking a simple transformation of random deviates from a beta distribution and dcayley evaluates the Cayley density at a given angle, r.

Finally the circular-von Mises-based distribution is included because the distribution is non-regular and has been applied to EBSD data (Bingham et al., 2009). An angle following this distribution has the distribution form

$$C_M(r|\kappa) = \frac{1}{2\pi I_0(\kappa)} e^{\kappa \cos(r)}.$$

Simulation from this distribution was developed by Best and Fisher (1979) and the function rvmises follows this procedure closely. Also, dvmises evaluates the density at a given angle, r.

Once an angular distribution has been chosen and a vector of n angles of rotation have been generated, the genR function with option space="SO3" creates an $n \times 9$ matrix representing a sample from the appropriate UARS member as demonstrated in the following code. If quaternions or Euler angles are desired the options space can be changed to "Q4" and "R3", respectively.

```
rs <- rcayley(20, 1)
Rs <- genR(rs)
R1 <- matrix(Rs[1, ], 3, 3)
is.SO3(R1)

## [1] TRUE
```

Here rcayley(20,1) simulates $r_1, \ldots, r_{20}$ from $C_C(r|\kappa = 1)$ then genR generates the matrices. Each row of Rs is an element in $SO(3)$, as demonstrated by is.SOn, in vector form with central orientation $I_{3\times3}$. Any other central orientation in $SO(3)$ is possible by changing the S option. If a central orientation not in $SO(3)$ is proposed, however, an error is returned.

$SO(3)$ **data analysis**

Given a sample of n observations $R_1, \ldots, R_n$ generated according to (1) we offer four ways to estimate the matrix S, i.e. the central orientation. These estimators are either Riemannian- or Euclidean-based in geometry and either mean- or median-based.

The choice of geometry results in two different metrics to measure the distance between rotation matrices R_1 and $R_2 \in SO(3)$. Under the embedding approach, the natural distance metric between two random matrices in the Euclidean distance, d_E, is induced by the Frobenius norm

$$d_E(R_1, R_2) = \|R_1 - R_2\|_F, \qquad (3)$$

where $\|A\|_F = \sqrt{\mathbf{tr}(A^\top A)}$ denotes the Frobenius norm of a matrix A and $\mathbf{tr}(\cdot)$ denotes the trace of a matrix. The Euclidean distance between two rotation matrices corresponds to the shortest cord in $\mathcal{M}(3)$ that connects them. If $r \in [0, \pi]$ denotes the misorientation angle in the angle-axis representation (2) of $R_1^\top R_2 \equiv R_1^\top R_2(r, U)$ (so that $\mathbf{tr}(R_1^\top R_2) = 1 + 2\cos r$), then $d_E(R_1, R_2) = 2\sqrt{(1 - \cos r)}$ holds.

By staying in the Riemannian space $SO(3)$ under the intrinsic approach, the natural distance metric becomes the Riemannian (or geodesic) distance, d_R, by which the distance between two rotations $R_1, R_2 \in SO(3)$ is defined as

$$d_G(R_1, R_2) = \frac{1}{\sqrt{2}} \|\mathrm{Log}(R_1^\top R_2)\|_F = \sin(r), \qquad (4)$$

where $\mathrm{Log}(R)$ denotes the principle logarithm of R (i.e., $\mathrm{Log}(R) = \mathrm{Log}(R(U, r)) = \Phi(rU)$ in (2)) and $r \in [0, \pi]$ is the misorientation angle of $R_1^\top R_2$. The Riemannian distance corresponds to the length of the shortest path that connects R_1 and R_2 *within* the space $SO(3)$. For this reason, the Riemannian distance is often considered the more natural metric on $SO(3)$; see Moakher (2002) for this discussion along with more details on exponential/logarithmic operators related to $SO(3)$.

We first consider estimators based on the embedding approach, which we call the projected estimators and denote with a subscript P. The median-based estimator in this class is

$$\widetilde{S}_P = \text{argmin}_{S \in SO(3)} \sum_{i=1}^{n} d_E(\boldsymbol{R}_i, \boldsymbol{S}). \qquad (5)$$

The function `rmedian` approximates $\widetilde{S}_P$ and uses an adaptation of the famous Weiszfeld algorithm (Weiszfeld, 1937). The mean-based estimator is

$$\widehat{S}_P = \text{argmin}_{S \in SO(3)} \sum_{i=1}^{n} d_E^2(\boldsymbol{R}_i, \boldsymbol{S})$$
$$= \text{argmax}_{S \in SO(3)} \text{tr}(\boldsymbol{S}^\top \bar{\boldsymbol{R}}) \qquad (6)$$

and is computed by the function `arith.mean`. For an in-depth discussion of the algorithm used to compute this value consult Moakher (2002).

The intrinsic estimators are referred to as geometric estimators and minimize the first and second order Riemannian distances. The *geometric median* is

$$\widetilde{S}_G = \text{argmin}_{S \in SO(3)} \sum_{i=1}^{n} d_G(\boldsymbol{R}_i, \boldsymbol{S}); \qquad (7)$$

and is computed by the function `HartleyL1`, which uses an algorithm proposed by Hartley et al. (2011). The mean-based counterpart is

$$\widehat{S}_G = \text{argmin}_{S \in SO(3)} \sum_{i=1}^{n} d_G^2(\boldsymbol{R}_i, \boldsymbol{S}). \qquad (8)$$

and is computed using the function `MantonL2` as proposed by Manton (2004).

Confidence Area Construction

With limited theory available for estimators of the central orientation, a bootstrap method is proposed to estimate the uncertainty associated with them. The procedure implemented by the function `CIradius` is as follows where $\widehat{S}$ is any of the estimators discussed so far:

1. Estimate $\widehat{S}$ from $(\boldsymbol{R}_1, \ldots, \boldsymbol{R}_n)$

2. Sample $\boldsymbol{R}_1,\ldots,\boldsymbol{R}_m$ from $(\boldsymbol{R}_1, \ldots, \boldsymbol{R}_n)$ with replacement

3. Estimate $\widehat{S}^*$ from bootstrap sample

4. Compute $\hat{T} = d_G(\widehat{S}, \widehat{S}^*)$

5. Repeat steps 1-3 B times

6. Report q% percentile of $\hat{T}$ to be the radius of the confidence 'cone'

A similar procedure was used by Bingham et al. (2010), but in place of d_R the maximum absolute angle between all three axis, which they called α, was used. It's easy to show that α is less than or equal to the geodesic distance between any two rotations making our method slightly more conservative.

Visualizations

In this section we introduce a method to visualize $SO(3)$ data via the the **ggplot2** package (Wickham, 2009). The function `eyeBall` takes as input a $n \times 9$ matrix of $SO(3)$ observations and returns a visualization of one of the three columns. The user can specify which column to use with the `column` option, the default is one.

The four estimates of the central orientation given in the previous section can be plotted by setting `estimates.show=TRUE`. The estimators are indicated by shape. One can also center the data about any observation in $SO(3)$ by setting `center=S`. Typically take `center=arith.mean(os)`.

```
rs <- rvmises(50, 0.01)
Rs <- genR(rs)
eyeBall(Rs, show.estimates = T)
```
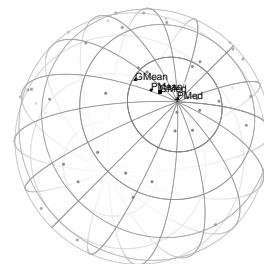

Figure 1: A plot of the a random sample from the von Mises-UARS distribution with $\kappa = 0.01$.

In figure 1 a random sample of 50 matrices following the von Mises UARS distribution with $\kappa = 0.01$ is plotted along with four estimates of the central orientation. The code to produce this plot is also given.

Summary

This file is only a basic article template. For full details of *The R Journal* style and information on how to prepare your article for submission, see the Instructions for Authors.

Bibliography

D. Best and N. Fisher. Efficient simulation of the von mises distribution. *Applied Statistics*, 28(2):152–157, 1979. ISSN 0035-9254.

M. Bingham, D. Nordman, and S. Vardeman. Modeling and inference for measured crystal orientations and a tractable class of symmetric distributions for rotations in three dimensions. *Journal of the American Statistical Association*, 104(488):1385–1397, 2009.

M. Bingham, D. Nordman, and S. Vardeman. Finite-sample investigation of likelihood and bayes inference for the symmetric von mises-fisher distribution. *Computational Statistics & Data Analysis*, 54 (5):1317–1327, 2010.

T. Downs. Orientation statistics. *Biometrika*, 59(3): 665–676, 1972.

R. Hartley, K. Aftab, and J. Trumpf. L1 rotation averaging using the weiszfeld algorithm. In *2011 IEEE Conference on Computer Vision and Pattern Recognition (CVPR)*, pages 3041–3048. IEEE, 2011.

P. Jupp and K. Mardia. Maximum likelihood estimators for the matrix von Mises-Fisher and Bingham distributions. *The Annals of Statistics*, 7(3):599–606, 1979. ISSN 0090-5364.

C. Khatri and K. Mardia. The von mises-fisher matrix distribution in orientation statistics. *Journal of the Royal Statistical Society. Series B (Methodological)*, 39(1):95–106, 1977. ISSN 0035-9246.

P. Langevin. Magnetism and the theory of the electron. *Annales de chimie et de physique*, 5:70, 1905.

C. León, J. Massé, and L. Rivest. A statistical model for random rotations. *Journal of Multivariate Analysis*, 97(2):412–430, 2006.

J. Manton. A globally convergent numerical algorithm for computing the centre of mass on compact lie groups. In *8th Conference on Control, Automation, Robotics and Vision, (ICARCV)*, volume 3, pages 2211–2216. IEEE, 2004.

M. Moakher. Means and averaging in the group of rotations. *SIAM Journal on Matrix Analysis and Applications*, 24(1):1–16, 2002.

H. Schaeben. A simple standard orientation density function: The hyperspherical de la vallée poussin kernel. *Phys. Stat. Sol. (B)*, 200:367–376, 1997.

E. Weiszfeld. Sur le point pour lequel la somme des distances de n points donnés est minimum. *Tohoku Mathematics Journal*, 43:355–386, 1937.

H. Wickham. *ggplot2: elegant graphics for data analysis*. Springer New York, 2009. ISBN 978-0-387-98140-6. URL http://had.co.nz/ggplot2/book.

Bryan Stanfill
Department of Statistics
Iowa State University
Ames, IA 50011
stanfill@iastate.edu

Heike Hofmann
Department of Statistics
Iowa State University
Ames, IA 50011
hofmann@mail.iastate.edu

Ulrike Genschel
Department of Statistics
Iowa State University
Ames, IA 50011
ulrike@mail.iastate.edu